Stanford Exploration Project, Report 124, April 4, 2006, pages 17–30

Stanford Exploration Project, Report 124, April 4, 2006, pages 17–30

Optimized implicit finite-difference migration for VTI media

Guojian Shan

ABSTRACT

I develop an implicit finite-difference migration method for vertical transversely isotropic (VTI) media with laterally varying anisotropy parameters. I approximate the dispersion relation of VTI media with a rational function series, the coefficients of which are estimated by least-squares optimization. These coefficients are functions of Thomsen anisotropy parameters. They are calculated and stored in a table before the wavefield extrapolation. The implicit finite-difference scheme for VTI media is almost the same as that of the isotropic media, except that the coefficients are derived from the pre-calculated table. In the 3D case, a phase-correction filter is applied after the finite-difference operator to eliminate the numerical-anisotropy error caused by two-way splitting. This finite-difference operator for VTI media is accurate to 60°, and its computational cost is almost the same as the isotropic migration. I apply this method to a 2D synthetic dataset and a 2D slice of a real 3D dataset to validate the method.

INTRODUCTION

Anisotropy is becoming increasingly important in seismic imaging. If anisotropy is not included in migration, reflectors will not be imaged at the right positions, or even worse, they will be defocused. However, imaging in a general anisotropic medium is still a challenging problem. A vertical transversely isotropic (VTI) medium is one of the simplest and most practical approximations for anisotropic media in seismic imaging. Compared to that of isotropic media, the dispersion relation of VTI media is much more complicated. As a result, phase-shift-based methods (Rousseau, 1997; Ferguson and Margrave, 1998) and explicit convolution methods (Uzcategui, 1995; Zhang et al., 2001a,b; Baumstein and Anderson, 2003; Shan and Biondi, 2005; Ren et al., 2005) are usually used in anisotropic migration, because the complex dispersion relation does not increase the difficulty of these algorithms. However, phase shift with interpolation requires a lot of reference wavefields, because there are two Thomsen anisotropy parameters in addition to the vertical velocity. Explicit convolution methods do not guarantee stability, and they also require long convolution filters to achieve good accuracy.

The implicit finite-difference method has been one of the most attractive migration methods for isotropic media. It can handle lateral variation naturally and guarantee stability. Traditional finite-difference methods, such as the 15° equation (Claerbout, 1971) and the 45° equation (Claerbout, 1985), approximate the dispersion relation by the truncation of Taylor series. Lee and Suh (1985) approximate the square-root equation with rational functions, and optimize the coefficient with least-squares. This can achieve a scheme accurate to 65^o. It is much more difficult to design an implicit finite-difference method for VTI media, because of the complicated dispersion relation. Under the weak anisotropy assumption, Ristow and Ruhl (1997) design an implicit scheme for VTI media. Liu et al. (2005) apply a phase-correction operator (Li, 1991) after the finite-difference operator for VTI media and improve the accuracy.

In this paper, I present an optimized one-way wave equation for VTI media and introduce a table-driven, implicit finite-difference method for laterally varying media. I also apply the phase-correction filter to reduce the error. I test the scheme with synthetic and real data.

OPTIMIZED ONE-WAY WAVE EQUATION OPERATOR FOR VTI

For isotropic media, the dispersion relation for the one-way wave equation can be represented as

$$\frac{k_z}{\omega/v} = \sqrt{1-\left(\frac{k_r}{\omega/v}\right)^2}, \tag{1}$$

where ω is the circular frequency, $v = v(x,y,z)$ is the velocity, k_z is the wavenumber, $k_r = \sqrt{k_x^2+k_y^2}$ is the radial wavenumber, and k_x, k_y are wavenumbers for x and y respectively. Let $S_z = \frac{k_z}{\omega/v}$, and $S_r = \frac{k_r}{\omega/v}$. The square-root function can be approximated by a series of rational functions:

$$S_z \approx 1 - \sum_{i=1}^{n} \frac{\alpha_i S_r^2}{1-\beta_i S_r^2}. \tag{2}$$

The coefficients α_i and β_i can be obtained by Taylor-series analysis or rational factorization. If we consider the second-order approximation ($n = 1$) and $\alpha_1 = \frac{1}{2}$, $\beta_1 = \frac{1}{4}$, we obtain the traditional 45° equation. The coefficients α_i and β_i can also be obtained by least-squares optimization, and a more accurate finite-difference scheme like the 65° equation can be obtained (Lee and Suh, 1985).

For VTI media, the true dispersion relation requires solving a quartic equation numerically (Shan and Biondi, 2005). With the assumption that the S-wave velocity is much smaller than the P-wave velocity, the dispersion relation for VTI media can be obtained analytically and represented as follows:

$$\frac{k_z}{\omega/v_p} = \sqrt{\frac{1-(1+2\varepsilon)\frac{k_r^2}{(\omega/v_p)^2}}{1-2(\varepsilon-\delta)\frac{k_r^2}{(\omega/v_p)^2}}}, \tag{3}$$

where $v_p = v_p(x,y,z)$ is the vertical velocity, and $\varepsilon = \varepsilon(x,y,z)$ and $\delta = \delta(x,y,z)$ are the anisotropy parameters defined by Thomsen (1986):

$$\varepsilon = \frac{C_{11}-C_{33}}{2C_{33}}, \delta = \frac{(C_{11}+C_{44})^2-(C_{33}-C_{44})^2}{2C_{33}(C_{33}-C_{44})},$$

where C_{ij} are elastic stiffness moduli. Let $S_z = \frac{k_z}{\omega/v_p}$ and $S_r = \frac{k_r}{\omega/v_p}$. This dispersion relation can be further simplified under the weak anisotropy assumption, and it can be approximated as

$$S_z \approx 1 - \frac{\alpha_1 S_r^2}{1-\beta_1 S_r^2}, \tag{4}$$

where $\alpha_1 = 0.5(1+2\delta)$ and $\beta_1 = \frac{2(\varepsilon-\delta)}{1+2\delta} + 0.25(1+2\delta)$ (Ristow and Ruhl, 1997). The coefficients α_1 and β_1 are obtained analytically by Taylor-series analysis.

As in the isotropic case, the coefficients α_i and β_i can also be obtained by least-squares optimization. The advantage of least-squares approximation is that I do not have to derive an explicit approximated expression for the dispersion relation analytically. This is especially useful for anisotropic media. For VTI media, I can use the true dispersion relation, and no assumption of small S-wave velocity and weak anisotropy is necessary.

Generally, the Padé approximation suggests that if the function $S_z(S_r) \in C^{n+m}$, then $S_z(S_r)$ can be approximated by a rational function $R_{n,m}(S_r)$:

$$R_{n,m}(S_r) = \frac{P_n(S_r)}{Q_m(S_r)}, \tag{5}$$

where

$$P_n(S_r) = \sum_{i=0}^{n} a_i S_r^i$$

and

$$Q_m(x) = \sum_{i=0}^{m} b_i S_r^i$$

are polynomials of degree n and m, respectively. The coefficients a_i and b_i can be obtained either analytically by Taylor-series analysis or numerically by least-squares fitting.

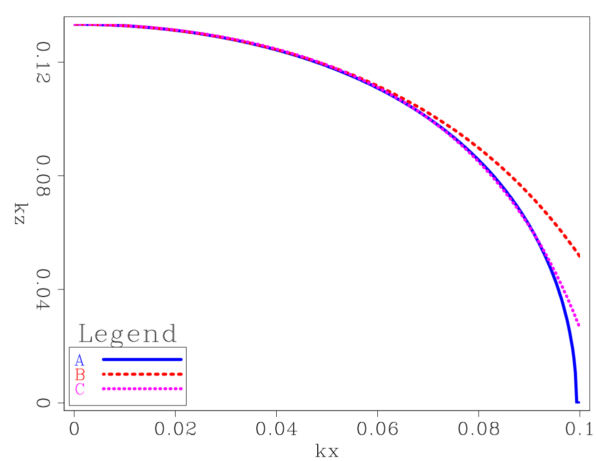

Figure 1: Dispersion relation: curve A is the true dispersion relation; B is the aprroximate dispersion relation by Tayor-series analysis; C is the approximate dispersion relation by optimization. guojian2-kz1 [ER]

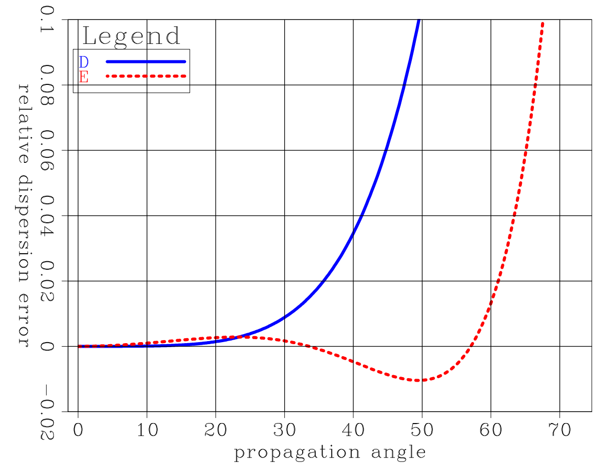

Figure 2: Relative dispersion error: curve D is the relative dispersion error of the approximation by Taylor-series analysis; E is the relative dispersion error of the approximation by optimization. guojian2-err1 [ER]

We can obtain the coefficients a_i and b_i by solving the following optimization problem:

$$\min \int_0^{\sin(\phi)} \left(\sqrt{\frac{1-(1+2\varepsilon)S_r^2}{1-2(\varepsilon-\delta)S_r^2}} - \frac{\sum a_i S_r^2}{\sum b_i S_r^2} \right)^2 dS_r, \tag{6}$$

where ϕ is the maximum optimization angle. This problem can be changed to

$$\min \int_0^{\sin(\phi)} \left(\sqrt{\frac{1-(1+2\varepsilon)S_r^2}{1-2(\varepsilon-\delta)S_r^2}} \left(\sum_{i=0}^{m} b_i S_r^2 \right) - \left(\sum_{i=0}^{n} a_i S_r^2 \right) \right)^2 dS_r. \tag{7}$$

The optimization problem (7) can be solved by a least-squares method. Given ε and δ, we can solve a_i and b_i from equation (7), and we can approximate k_z as follows:

$$k_z \approx \frac{\omega}{v_p} \frac{\sum_{i=0}^{n} a_i S_r^i}{\sum_{i=0}^{m} b_i S_r^i}. \tag{8}$$

As Ma (1981) suggested, if $m = n$, equation (8) can be further split into a rational-function series as follows:

$$k_z \approx \frac{\omega}{v_p} \left(1 - \sum_{i=1}^{n} \frac{\alpha_i S_r^2}{1-\beta_i S_r^2} \right). \tag{9}$$

The dispersion error of approximation (9) is given by

$$\Delta k_z = \frac{\omega}{v_p} \left[\sqrt{\frac{1-(1+2\varepsilon)S_r^2}{1-2(\varepsilon-\delta)S_r^2}} - \left(1 - \sum_{i=1}^{n} \frac{\alpha_i S_r^2}{1-\beta_i S_r^2} \right) \right]. \tag{10}$$

The relative dispersion error is defined by $\Delta k_z / k_z$.

For the second-order approximation ($m = 1, n = 1$), Figure 1 shows the true and approximated dispersion relation, given $\varepsilon = 0.4$ and $\delta = 0.2$. In Figure 1, curve A is the true dispersion relation curve. B is the approximated dispersion suggested by Ristow and Ruhl (1997), in which $\alpha_1 = 0.700000$ and $\beta_1 = 0.635714$. C is the approximated dispersion relation by the least-squares optimization, in which $\alpha_1 = 0.664820$ and $\beta_1 = 0.948380$. The dispersion relation by optimization (C) approximates the true dispersion relation better than the approximation using Taylor-series analysis and the weak anisotropy assumption.

Figure 2 shows the relative dispersion error. D is the relative dispersion error of the approximation using the Taylor-series analysis. E is the relative dispersion error of the optimized one-way wave operator. Figure 2 shows that opimization greatly improves the dispersion relation. If we accept a one-percent dispersion error, the optimized one-way wave-equation is accurate to 60° while the approximation using Taylor-series analysis is accurate to only 30°.

TABLE-DRIVEN IMPLICIT FINITE-DIFFERENCE MIGRATION

For the second-order approximation ($m = 1, n = 1$), equation (9) is the following cascaded partial differential equation in the space domain:

$$\frac{\partial}{\partial z}P = i\frac{\omega}{v_p}P, \tag{11}$$

$$\frac{\partial}{\partial z}P = i\frac{\omega}{v_p}\frac{\alpha_1 \frac{v_p^2}{\omega^2}(\frac{\partial^2}{\partial x^2} + \frac{\partial^2}{\partial y^2})}{1 + \beta_1 \frac{v_p^2}{\omega^2}(\frac{\partial^2}{\partial x^2} + \frac{\partial^2}{\partial y^2})}P. \tag{12}$$

In isotropic migration, α_1 and β_1 are constant. In VTI media, α_1 and β_1 are functions of the anisotropy parameters ε and δ. For laterally varying media, the value of α_1 and β_1 also vary laterally. It is too expensive to calculate α_1 and β_1 for each grid point during the wavefield extrapolation. I calculate α_1 and β_1 for a range of ε and δ and store them in a table before the migration. I then generate maps of α_1 and β_1 from the table. With the map of the coefficents α_1 and β_1, the finite-difference scheme for VTI media can be performed in the same way as an isotropic migration.

PHASE CORRECTION FILTER

In the 3D case, as in the isotropic migration, the dispersion relation is split into x and y components as follows:

$$\frac{\partial}{\partial z}P = i\frac{\omega}{v_p}\left[\frac{\alpha_1 \frac{v_p^2}{\omega^2}\frac{\partial^2}{\partial x^2}}{1 + \beta_1 \frac{v_p^2}{\omega^2}\frac{\partial^2}{\partial x^2}} + \frac{\alpha_1 \frac{v_p^2}{\omega^2}\frac{\partial^2}{\partial y^2}}{1 + \beta_1 \frac{v_p^2}{\omega^2}\frac{\partial^2}{\partial y^2}}\right]P. \tag{13}$$

This two-way splitting causes numerical anisotropy, which can be remedied by a phase-correction filter (Li, 1991) in the Fourier domain as follows:

$$P = Pe^{i\Delta z k_L}, \tag{14}$$

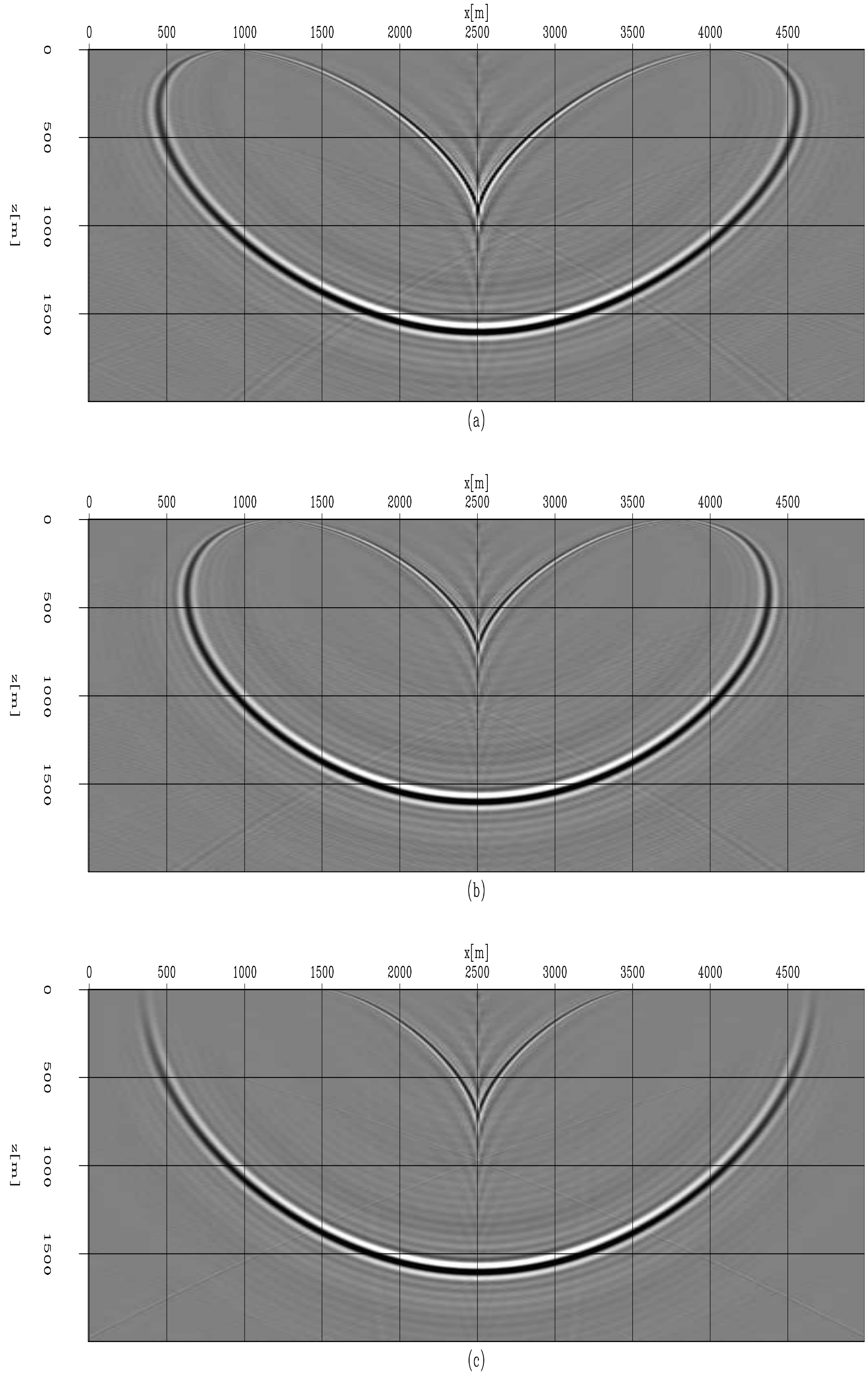

Figure 3: Impulse responses: (a) Optimized finite-difference method; (b) Finite-difference method by Tayor-series analysis; (c) Phase-shift method. guojian2-impulse [CR]

where

$$k_L = \sqrt{\frac{1-(1+2\varepsilon_r)\frac{k_r^2}{(\omega/v_p^r)^2}}{1-2(\varepsilon_r-\delta_r)\frac{k_r^2}{(\omega/v_p^r)^2}}} - \left[1 - \frac{\alpha_1^r(\frac{\omega}{v_p^r}k_x)^2}{1-\beta_1^r(\frac{\omega}{v_p^r}k_x)^2} - \frac{\alpha_1^r(\frac{\omega}{v_p^r}k_y)^2}{1-\beta_1^r(\frac{\omega}{v_p^r}k_y)^2}\right], \tag{15}$$

where v_p^r is the reference vertical velocity, ε_r and δ_r are the reference anisotropy parameters, and α_1^r and β_1^r are the optimized finite-difference coefficients corresponding to the anisotropy parameters ε_r and δ_r.

NUMERICAL EXAMPLES

Impulse response

Figure 3 shows the impulse responses of a homogeneous VTI medium. The vertical velocity of the medium is 2000 m/s, the anisotropy parameter ε is 0.4 and the anisotropy parameter δ is 0.2. The travel-time of the impulse is 2 seconds. Figure 3(a) is the impulse response of the optimized implicit finite-difference operator, Figure 3(b) is the impulse response of the finite-difference operator by Taylor-series analysis suggested by Ristow and Ruhl (1997), and Figure 3(c) is the impulse response of the phase-shift operator, using equation (3) as the dispersion relation. Comparing these three impulse responses, we can see that the impulse response of the optimized implicit finite-difference operator (Figure 3(a)) is more accurate than the impulse response from Taylor-series analysis (Figure 3 (b)). The impulse response in Figure 3(a) is accurate to 60°, while the impulse response in Figure 3(b) is accurate to only 30°. The impulse responses also verify the relative-dispersion-relation error analysis in Figure 2.

A synthetic dataset

Figures 4-6 show a synthetic model for VTI media. Figure 4 is the velocity model, Figure 5 is the map of the anisotropy parameter ε, and Figure 6 is the map of the anisotropy parameter δ. There are 720 shots in total and the maximum offset for each shot is 8000 meters. The challenging part of this model is to accurately image the steep fault, salt flank and the two abnormal sediments near the right corner of the salt body. I run a plane-wave migration, using the optimized implicit finite-difference operator as the extrapolator. I generate 70 plane-wave sources, for which the take-off angles at the surface range from $-40°$ to $40°$. Figure 7 shows the image. Notice that the steeply dipping salt flank and the fault are well imaged. The steepest part of the salt flank is about 60°. The abnormal sediments also are well imaged.

A real dataset: ExxonMobil MC311

Figures 8 and 9 show the map of two anisotropy parameters, ε and δ, for a 2D slice of the real dataset MC311. Notice the strong anisotropic layers around the salt body. Figure 10 shows the

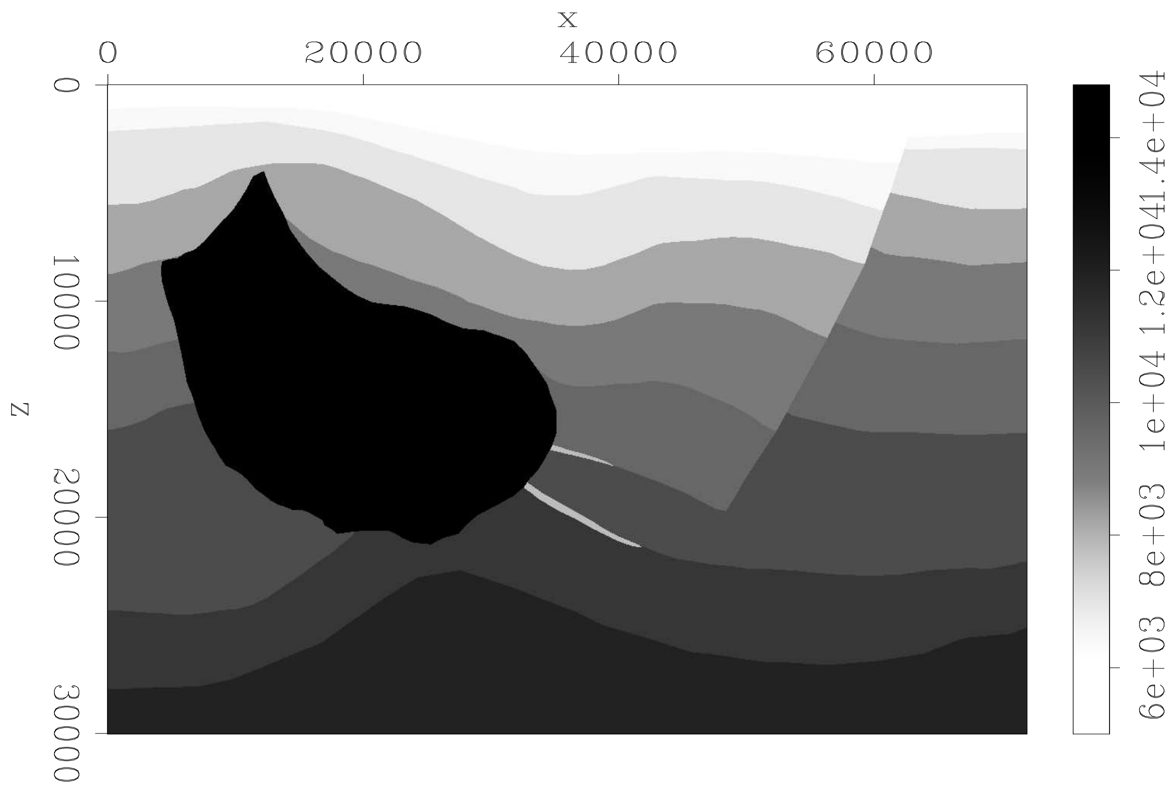

Figure 4: Vertical velocity model. guojian2-vpani [ER]

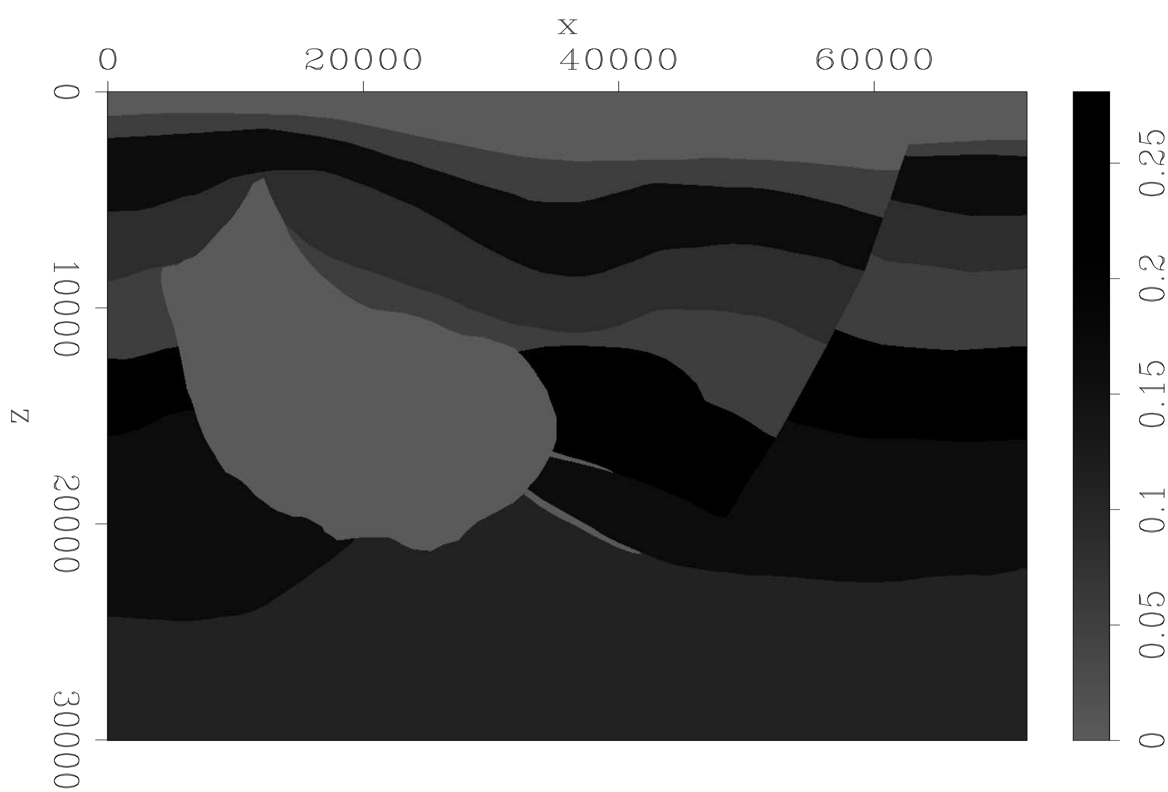

Figure 5: Anisotropy parameter ε. guojian2-epsani [ER]

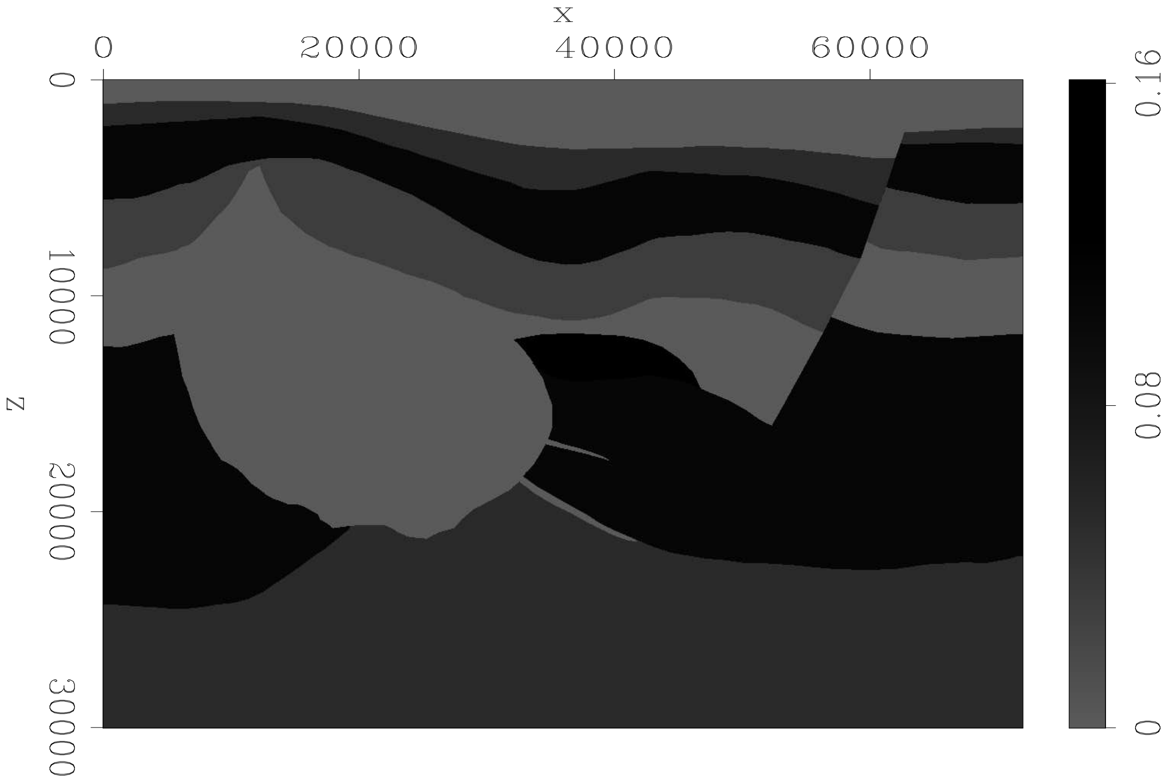

Figure 6: Anisotropy parameter δ. guojian2-dltani [ER]

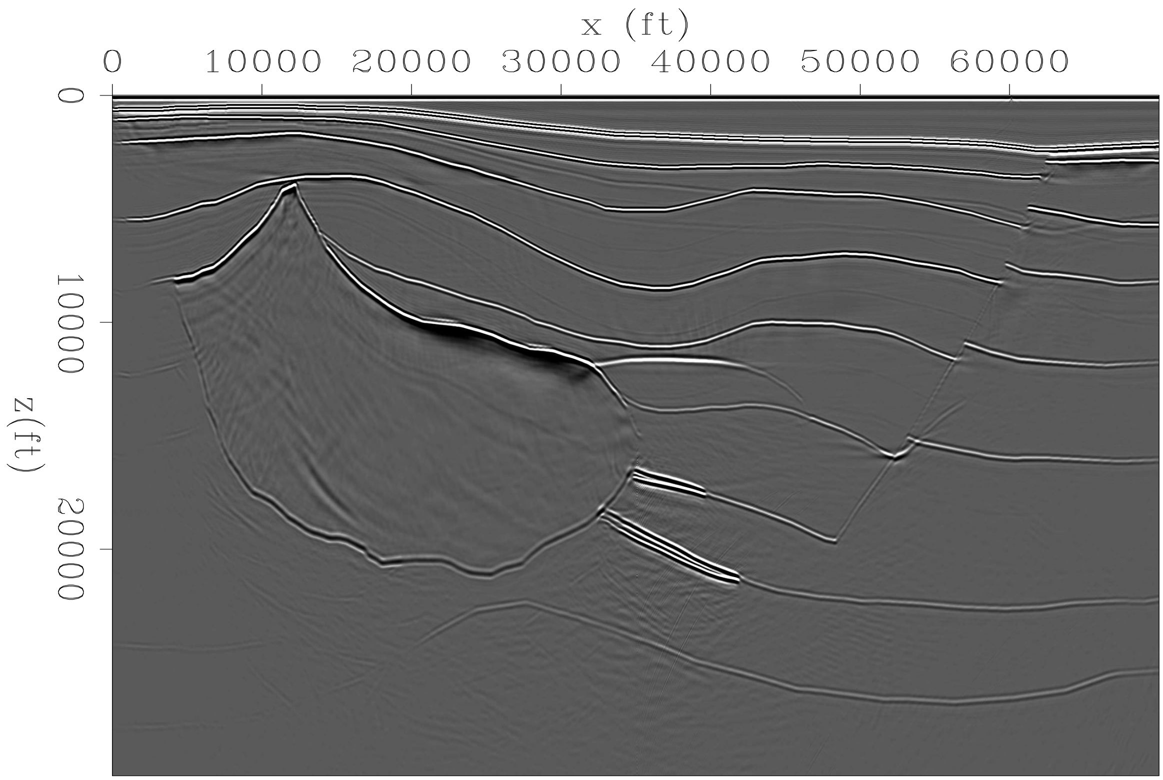

Figure 7: Implicit finite-difference migration. guojian2-imfdhess [CR]

image obtained by plane-wave migration, using the optimized implicit finite-difference operator as the extrapolator. The steeply dipping sediments around the salt below the anisotropic layers are well imaged. Figure 11 shows the image obtained by plane-wave migration, using an implicit isotropic operator plus a 5 point explicit anistropic correction filter (Shan and Biondi, 2005) as the extrapolator. The two images are comparable, while the implicit finite-difference method is much cheaper.

CONCLUSION

I present an implicit finite-difference migration method for VTI media. The scheme is designed by approximating the dispersion relation with rational functions and solving the coefficients by least-squares methods. The coefficients of finite-difference are obtained from a table, which is calculated before the wavefield extrapolation. This implicit finite-difference method guarantees stability, and its computational cost is almost the same as isotropic implicit finite-difference migration. Both dispersion-error analysis and impulse response indicate that the implicit finite-difference operator is accurate to 60°. The migrations for the synthetic and real datasets show that this implicit finite-difference method can extrapolate the wavefield accurately in laterally varying media.

ACKNOWLEDGMENTS

I would like to thank Faqi Liu from Amerada Hess for useful discussions. I would like to thank Amerada Hess for making the synthetic dataset available and ExxonMobil for making the real dataset available.

REFERENCES

Baumstein, A., and Anderson, J., 2003, Wavefield extrapolation in laterally varying VTI media *in* 73rd Ann. Internat. Mtg. Soc. of Expl. Geophys., 945–948.

Claerbout, J. F., 1971, Toward a unified theory of reflector mapping: Geophysics, **36**, 467–481.

—, 1985, Imaging the Earth's Interior: Blackwell Scientific Publications.

Ferguson, R. J., and Margrave, G. F., 1998, Depth migration in TI media by nonstationary phase shift *in* 68th Ann. Internat. Mtg. Soc. of Expl. Geophys., 1831–1834.

Lee, M. W., and Suh, S. Y., 1985, Optimization of one-way wave-equations (short note): Geophysics, **50**, 1634–1637.

Li, Z., 1991, Compensating finite-difference errors in 3-D migration and modeling: Geophysics, **56**, 1650–1660.

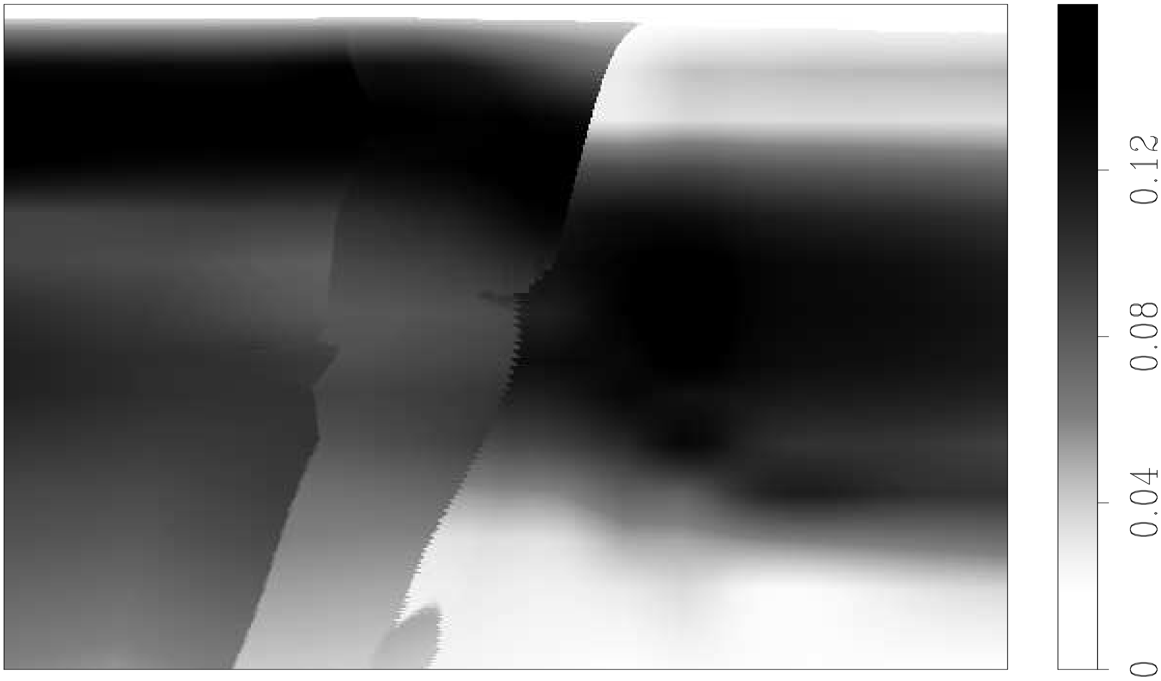

Figure 8: Anisotropy parameter ε. guojian2-epsex7000 [ER]

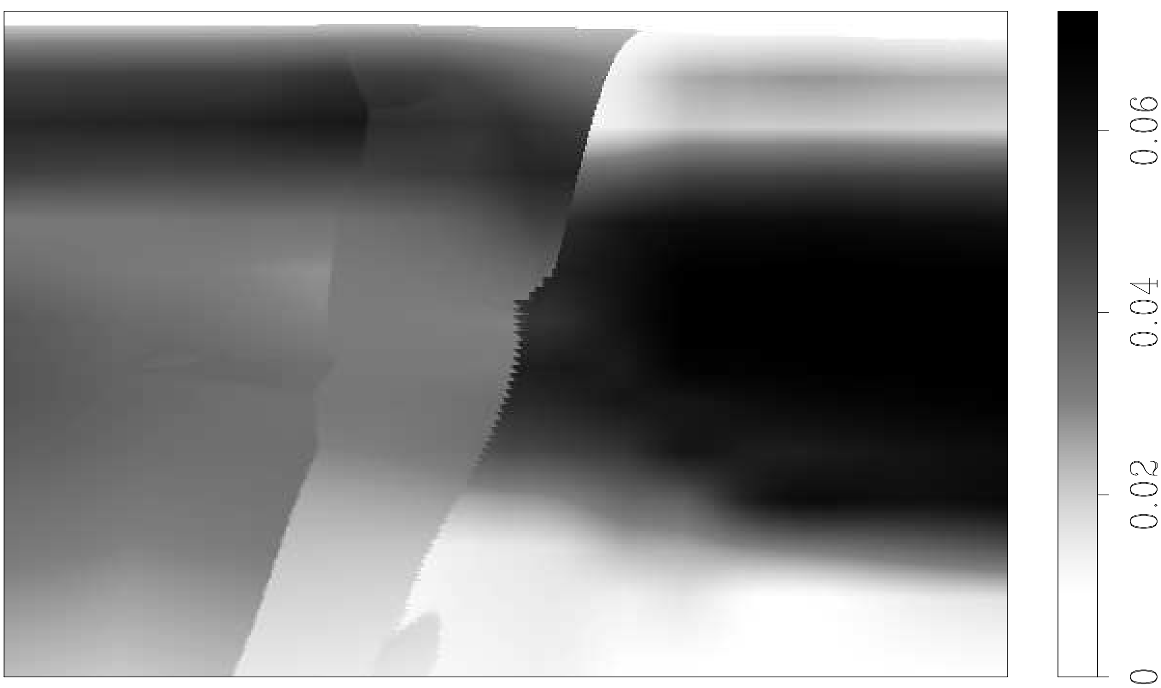

Figure 9: Anisotropy parameter δ. guojian2-dltex7000 [ER]

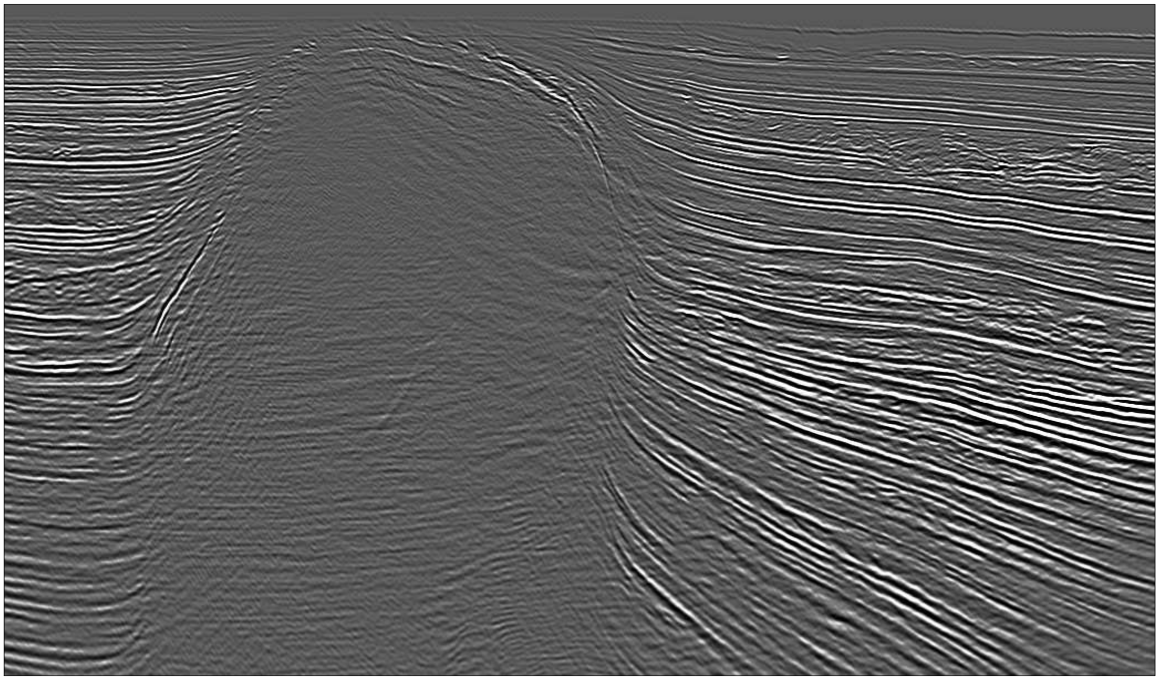

Figure 10: Implicit finite-difference migration. guojian2-imfdex7000 [CR]

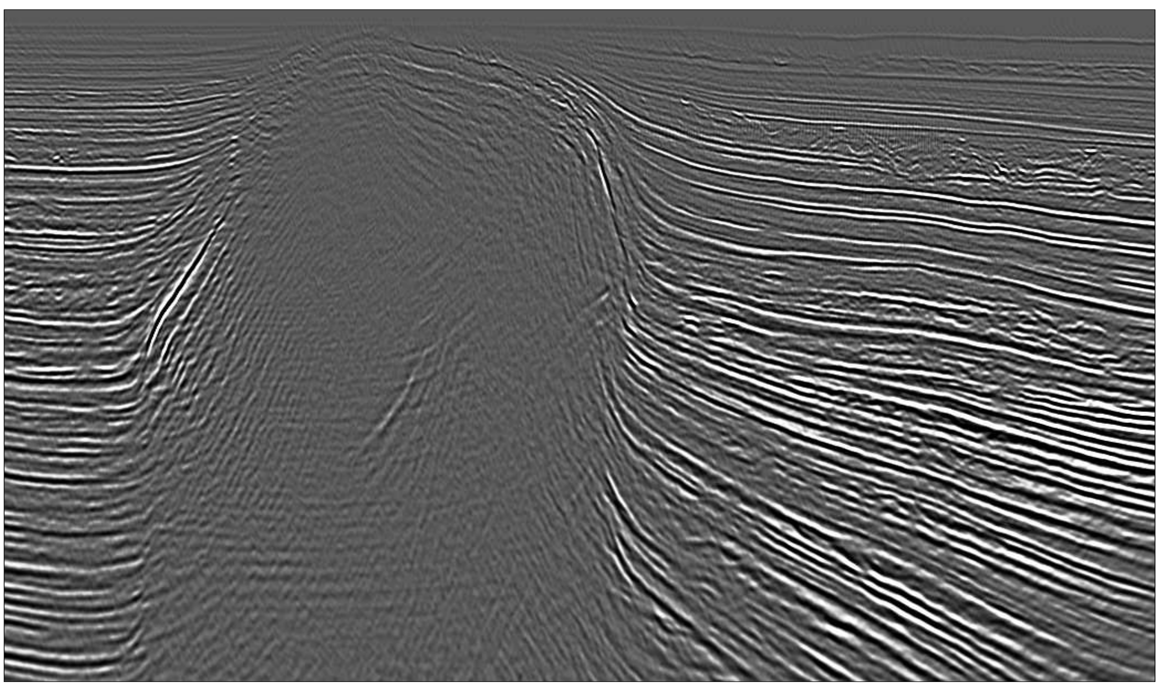

Figure 11: migration with an isotropic operator plus an explicit anisotropic correction filter. guojian2-exfdex7000 [CR]

Liu, F., Day, R., Hanson, D., Whitmore, D., Mosher, C., and Sinton, J., 2005, A stable wave equation migration method in 3D VTI media: 67th Ann. Internat. Mtg., EAGE, Expanded Abstracts, P002.

Ma, Z., 1981, Finite-difference migration with higher-order approximation: 1981 joint meeting of the China Geophysical Society and Soc. of Expl. Geophys., Beijing China.

Ren, J., Gerrard, C., McClean, J., and Orlovich, M., 2005, Wave equation prestack depth migration in laterally varying VTI media: 75th Ann. Internat. Mtg., Soc. of Expl. Geophys., Expanded Abstracts, 104–107.

Ristow, D., and Ruhl, T., 1997, Migration in transversely isotropic media using implicit operators *in* 67th Ann. Internat. Mtg. Soc. of Expl. Geophys., 1699–1702.

Rousseau, J. H. L., 1997, Depth migration in heterogeneous, transversely isotropic media with the phase-shift-plus-interpolation method *in* 67th Ann. Internat. Mtg. Soc. of Expl. Geophys., 1703–1706.

Shan, G., and Biondi, B., 2005, 3D wavefield extrapolation in laterally-varying tilted TI media: 75th Ann. Internat. Mtg., Soc. of Expl. Geophys., Expanded Abstracts, 104–107.

Thomsen, L., 1986, Weak elastic anisotropy: Geophysics, **51**, 1954–1966.

Uzcategui, O., 1995, 2-D depth migration in transversely isotropic media using explicit operators: Geophysics, **60**, 1819–1829.

Zhang, J., Verschuur, D. J., and Wapenaar, C. P. A., 2001a, Depth migration of shot records in heterogeneous, tranversely isotropic media using optimum explicit operators: Geophys. Prosp., **49**, 287–299.

Zhang, J., Wapenaar, C., and Verschuur, D., 2001b, 3-D depth migration in VTI media with explicit extrapolation operators *in* 71st Ann. Internat. Mtg. Soc. of Expl. Geophys., 1085–1088.